


Article

Anti-Pulmonary Fibrosis Activities of Triterpenoids from *Oenothera biennis*

Juanjuan Liu^{1,2}, Jingke Zhang^{1,2}, Mengnan Zeng^{1,2}, Meng Li^{1,2} , Shuangshuang Xie^{1,2}, Xiaoke Zheng^{1,2} and Weisheng Feng^{1,2,*}

¹ College of Pharmacy, Henan University of Chinese Medicine, Zhengzhou 450046, China; 118638238805@163.com (J.L.); 18137802812@163.com (J.Z.); 17320138484@163.com (M.Z.); limeng31716@163.com (M.L.); shuangxie@hactcm.edu.cn (S.X.); zhengxk.2006@163.com (X.Z.)

² The Engineering and Technology Center for Chinese Medicine Development of Henan Province, Zhengzhou 450046, China

* Correspondence: fwsh@hactcm.edu.cn

Abstract: Five new triterpenoids, oenotheralanosterols C-G (1–5), with seven known triterpenoid-compounds, namely 2 α ,3 α ,19 α -trihydroxy-24-norurs4,12-dien-28-oic acid (6), 3 β ,23-dihydroxy-1-oxo-olean-12-en-28-oic acid (7), remangilone C (8), Knoxivalic acid A (9), termichebulolide (10), rosasecotriterpene A (11), androsanortriterpene C (12), were extracted and separated from the dichloromethane part of *Oenothera biennis* L. The anti-pulmonary fibrosis activities of all the compounds against TGF- β 1-induced damage tonormal human lung epithelial (BEAS-2B) cells were investigated in vitro. The results showed that compounds 1–2, 6, 8, and 11 exhibited significant anti-pulmonary fibrosis activities, with EC₅₀ values ranging from 4.7 μ M to 9.9 μ M.

Keywords: *Oenothera biennis* L.; triterpenoids; anti-pulmonary fibrosis activities; BEAS-2B cells; RTCA



Citation: Liu, J.; Zhang, J.; Zeng, M.; Li, M.; Xie, S.; Zheng, X.; Feng, W. Anti-Pulmonary Fibrosis Activities of Triterpenoids from *Oenothera biennis*. *Molecules* **2022**, *27*, 4870. <https://doi.org/10.3390/molecules27154870>

Academic Editors: Kemal Husnu Can Baser and Stefano Dall'Acquaand

Received: 24 May 2022

Accepted: 25 July 2022

Published: 29 July 2022

Publisher's Note: MDPI stays neutral with regard to jurisdictional claims in published maps and institutional affiliations.



Copyright: © 2022 by the authors. Licensee MDPI, Basel, Switzerland. This article is an open access article distributed under the terms and conditions of the Creative Commons Attribution (CC BY) license (<https://creativecommons.org/licenses/by/4.0/>).

1. Introduction

Pulmonary fibrosis (PF) is an end-stage change of a large group of lung diseases which can lead to death if it is not properly treated [1]. The main causes of PF are the inhalation of foreign particles (such as dust and asbestos fibers), infections (such as COVID-19), autoimmune diseases (such as systemic autoimmune diseases of the connective tissue), and exposure to radiation treatment (such as radiation therapy for lung or breast cancer) [2]. Currently, PF is mainly conventionally treated using anti-inflammatory and immunosuppressant drugs (such as pirfenidone and nintedanib). However, these drugs can only retard the progression and relieve the symptoms of PF [3]. At the same time, an increasing number of Traditional Chinese Medicine therapies have been proven effective in treating PF [4–7]. Particularly, triterpenoids were proven to be bioactive structures against PF [8].

Oenothera is a genus that includes more than 200 species that are distributed in various regions of the world. These species can be found in the southern parts (northeast) and mountainous areas of China [9]. These species of *Oenothera biennis* are rich in a variety of natural compounds, including flavonoids, tannins, fatty acids, and terpenoids [10–14]. Modern pharmacological research has shown that these species possess antibacterial, anti-inflammatory, antioxidant, blood lipid lowering, blood sugar lowering, and anti-tumor properties, as well as other pharmacological effects [15–21]. Among these species, *Oenothera biennis* is a perennial herbaceous plant which is commonly used in folk medicine [22]. In consulting local books, we found that *O. biennis* can be used to treat lung-related diseases. For example, “Quanzhou Materia Medica” recorded that *O. biennis* can be used to treat lung disease and fistulas. Meanwhile, according to the literature, it is found that the triterpenoids in evening primrose have antiproliferative, antimicrobial efficacy, with free radical scavenging and ferric reducing activities [12,23]. In this study, we investigated and identified five new (1–5) and seven known triterpenoids (6–12) from the dichloromethane

fraction of *O. biennis* (Figure 1). Furthermore, some compounds have shown significant protective effects against TGF- β 1-induced PF in healthy human lung epithelial (BEAS-2B) cells, which suggests the potential anti-pulmonary fibrosis activities of these compounds.

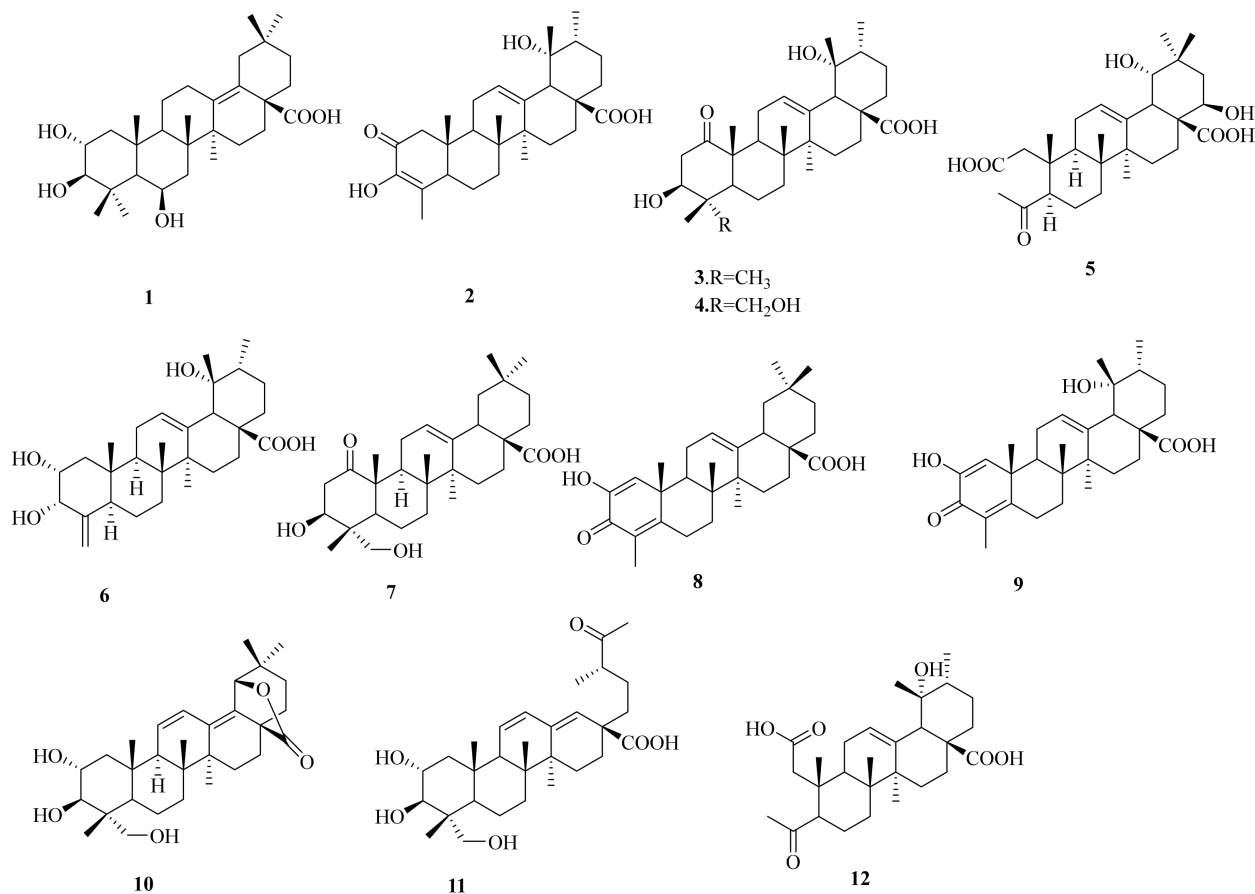


Figure 1. Structures of triterpenoids 1–12.

2. Results and Discussion

Compound 1 (Figure 1) was isolated as a white amorphous powder (20.6 mg), and the molecular formula was determined as C₃₀H₄₈O₅, based on the quasi-molecular ion at m/z 511.3397 [M + Na]⁺ (calculated for C₃₀H₄₈O₅Na, 511.3399) in the HR-ESI-MS. The IR absorption bands confirmed the presence of -OH (3369 cm⁻¹) and -COOH (1636 cm⁻¹) in compound 1. The UV spectrum exhibited an absorption band at λ 206 nm corresponding to the carbonyl group. The ¹H NMR spectrum (Table 1) showed three oxygenated methines at [δ_H 4.45 (1H, m, H-6), 3.70 (1H, m, H-2), and 2.86 (1H, d, J = 9.5 Hz, H-3)] and seven methyl groups at [δ_H 0.77 (3H, s, H-30), 0.93 (3H, s, H-29), 1.07 (3H, s, H-23), 1.16 (3H, s, H-24), 1.17 (3H, s, H-27), 1.17 (3H, s, H-26), and 1.32 (3H, s, H-25)]. The ¹³C NMR (Table 2) and DEPT 135 spectra exhibited 29 carbon resonances, including a carboxylic carbon at (δ_C 180.6), two olefinic carbons at (δ_C 139.1 and 129.8), three oxygenated methine carbons at (δ_C 68.8, 69.8, and 84.7), and seven methyl carbons at (δ_C 32.7, 28.8, 24.7, 21.8, 19.8, 19.5, and 18.7). The HMBC and ¹H–¹H COSY correlations of compound 1 are shown in Figure 2. The ¹H–¹H COSY spectrum, including δ_H 1.61, 1.52 (H-11), δ_H 1.62 (H-9), δ_H 2.81, and 1.88 (H-12), was consistent with a double bond in ring D. Meanwhile, it can be observed that the attachment of a double bond of C-13 and C-18 was established by HMBC correlations from δ_H 1.17 (H₃-27) to δ_C 139.1 (C-13) and from δ_H 2.27 (H-19) to δ_C 129.5 (C-18). The analysis of the ¹³C NMR data of compound 1 established its close structural resemblance to α , 3 β -dihydroxy-yolean-13(18)-en-28-oic acid [24]; however, the only difference was the presence of an oxygenated methine δ_C 68.8 (C-6) in compound 1 and the absence of a

methylenesignal compared to 2α , 3β -dihydroxy-yolean-13(18)-en-28-oic acid. The HMBC correlations from δ_{H} 4.45 (H-6) to δ_{C} 56.8 (C-5), δ_{C} 43.1 (C-7), and δ_{C} 39.3 (C-10) were observed. The relative configuration of compound **1** was determined based on a NOESY experiment. The NOESY correlation (Figure 3) was observed between H-2 and H₃-25, which indicated the α -orientation of the hydroxy group at C-2. The correlations of H-3 and H-5 demonstrated the α -orientation of H-3, which indicated that the hydroxy group at C-3 was β -oriented. Additionally, the NOESY correlation was observed between H-6 and H₃-23/H-5, which indicated that the hydroxy group at C-6 was β -oriented [25,26]. Thus, the structure of compound **1** was determined to be $2\alpha,3\beta,6\beta$ -trihydroxy-yolean-13(18)-en-28-oic acid, and it was named oenotheralanosterol C.

Table 1. H NMR data (500 MHz) for compounds 1–5 (δ , ppm, J , Hz) in CD₃OD.

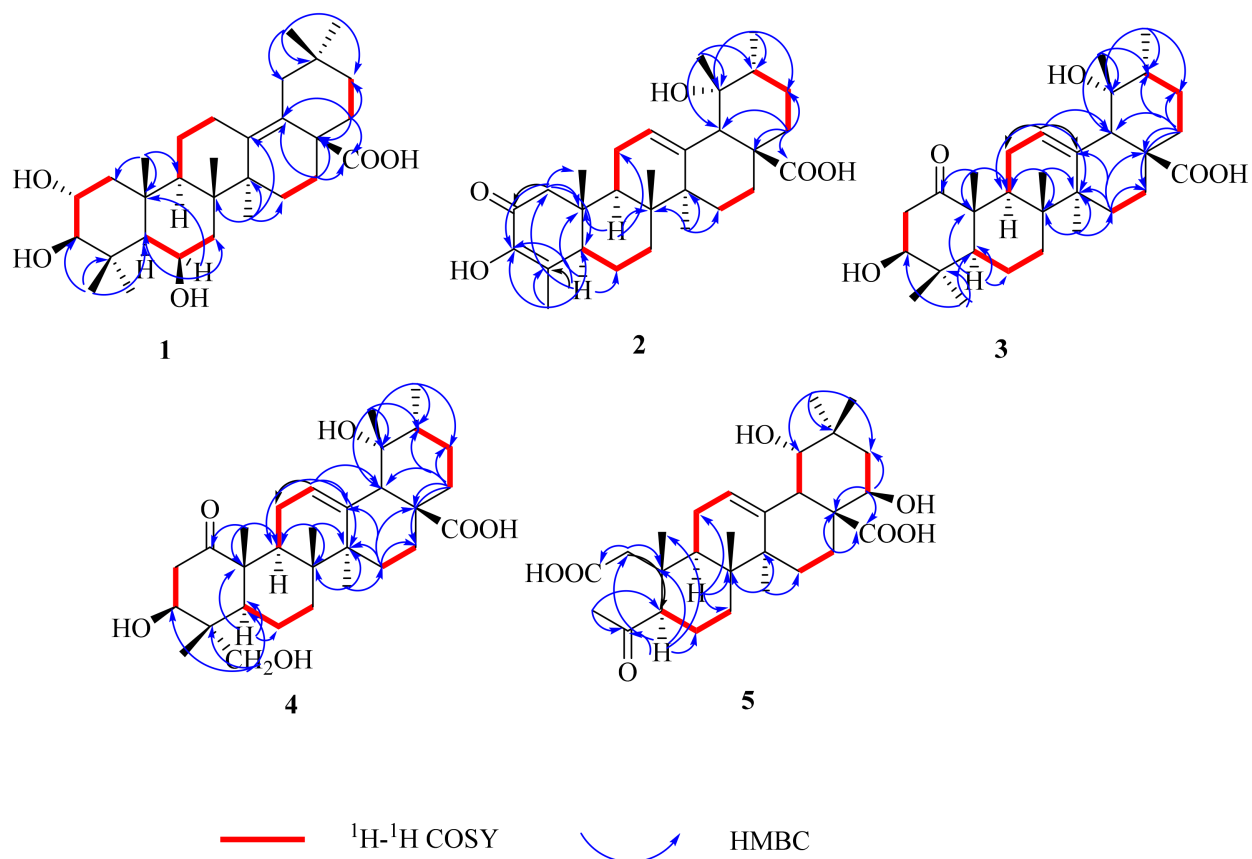
Position	1	2	3	4	5
1	2.04 <i>dd</i> (4.8, 12.4), 0.90 m	2.56 <i>d</i> (16.4)	-	-	2.36 s, 2.22 s
2	3.70 m	-	3.10 t (4.6), 2.26 <i>dd</i> , (4.6, 12.1)	3.11 m, 2.30 m	-
3	2.86 <i>d</i> (9.5)	-	3.36 <i>dd</i> (4.6, 12.1)	3.82 <i>dd</i> (4.9, 12.1)	-
4	-	-	-	-	-
5	0.83 <i>d</i> (2.0)	2.42 m	0.90 m	1.40 m	3.06 <i>dd</i> (3.0, 12.4)
6	4.45 m	1.90 m, 1.48 m	1.68 m, 1.61 m	1.60 m, 1.53 m	1.76 m, 1.67 m
7	1.64 m, 1.63 m	1.73 m, 1.43 m	1.51 m, 1.39 m	1.59 m, 1.30 m	1.59 m, 1.36 m
8	-	-	-	-	-
9	1.62 m	2.08 m	2.34 m	2.39 m	2.33 m
10	-	-	-	-	-
11	1.61 m, 1.52 m	2.07 m, 2.02 m	1.88 m, 1.54 m	2.46 m, 1.90 m	2.19 m, 2.04 m
12	2.82 m, 1.88 m	5.28 t (3.8)	5.27 t (3.6)	5.27 t (3.0)	5.35 t (3.8)
13	-	-	-	-	-
14	-	-	-	-	-
15	1.14 m, 1.06 m	1.81 m, 1.06 m	1.82 m, 1.76 m	1.78 m, 1.02 m	1.70 m, 1.11 m
16	1.91 m, 1.55 m	2.71 m, 1.57 m	2.57 m, 2.44 m	2.57 m, 2.45 m	2.00 m, 1.97 m
17	-	-	-	-	-
18	-	2.76 s	2.50 s	2.50 s	2.76 brs
19	2.47 <i>dd</i> , 1.76 <i>dd</i> (2.2, 14.0)	-	-	-	3.22 <i>d</i> (3.8)
20	-	1.69 m	1.34 m	1.32 m	-
21	1.28 m, 1.23 m	2.31 m, 1.19 m	1.75 m, 1.26 m	1.73 m, 1.25 m	1.80 m, 1.22 m
22	2.15 m, 1.34 m	1.84 m, 1.55 m	1.77 m, 1.63 m	1.72 m, 1.63 m	3.91 <i>dd</i> (4.4, 11.6)
23	1.07 s	1.85 <i>d</i> (2.0)	1.01 s	3.35 <i>d</i> , 3.51 <i>d</i> (11.2)	2.23 s
24	1.17 s	-	1.04 s	0.88 s	-
25	1.32 s	0.93 s	1.32 s	1.35 s	1.09 s
26	1.16 s	0.85 s	0.86 s	0.86 s	0.84 s
27	1.17 s	1.39 s	1.36 s	1.37 s	1.34 s
28	-	-	-	-	-
29	0.93 s	1.14 s	1.22 s	1.22 s	0.97 s
30	0.77 s	1.00 <i>d</i> (6.6)	0.94 <i>d</i> (6.7)	0.94 <i>d</i> (6.6)	1.03 s

Table 2. ¹³C NMR data (125 MHz) for compounds 1–5 (δ , ppm, J , Hz) in CD₃OD.

Position	1	2	3	4	5
1	50.5	53.2	215.3	215.3	44.4
2	69.8	195.7	45.1	44.8	175.4
3	84.7	145.3	79.7	73.4	-
4	41.1	133.1	40.4	44.1	215.6
5	56.8	49.9	55.8	47.7	57.5
6	68.8	22.0	19.0	18.6	23.1
7	43.1	33.2	34.1	33.6	32.2
8	41.6	40.6	40.9	40.8	43.3
9	52.6	44.9	40.1	40.0	40.8
10	39.3	42.3	53.8	53.3	40.6

Table 2. Cont.

Position	1	2	3	4	5
11	23.0	24.8	26.6	26.6	24.6
12	26.5	128.1	130.0	130.0	125.1
13	139.1	140.0	139.4	139.4	143.8
14	45.9	42.9	42.8	42.9	40.6
15	28.2	29.5	29.6	29.6	29.0
16	34.2	27.2	26.5	26.5	20.8
17	49.4	49.0	49.3	49.3	53.0
18	129.8	48.0	55.3	55.3	46.4
19	42.0	74.2	73.5	73.5	82.0
20	33.6	43.3	43.1	43.1	36.8
21	38.0	25.2	27.3	27.3	38.0
22	36.9	32.8	38.9	38.9	72.4
23	28.8	13.4	16.6	66.0	31.6
24	18.7	-	29.0	13.3	-
25	19.5	14.4	15.4	15.9	18.4
26	19.8	17.7	18.1	18.1	17.5
27	21.8	24.5	24.8	24.8	25.2
28	180.6	182.2	182.2	182.2	180.7
29	32.7	29.5	27.0	27.0	28.8
30	24.7	16.2	16.6	16.6	26.2

Figure 2. Key ^1H - ^1H COSY and HMBC correlations of compounds 1–5.

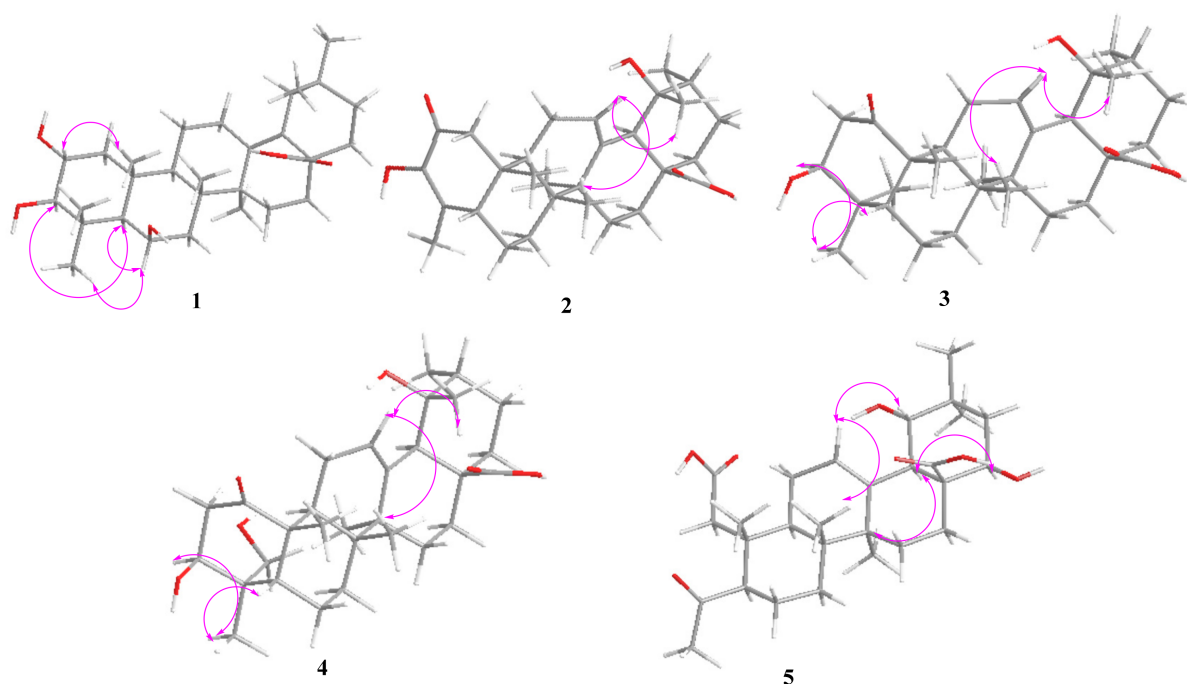


Figure 3. Key NOESY correlations of compounds 1–5.

Compound **2** (Figure 1) was isolated as a white amorphous powder (11.0 mg), and its molecular formula was established as $C_{29}H_{42}O_5$ from the molecular ion peak at m/z 493.2934 $[M + Na]^+$ (calculated for $C_{29}H_{42}O_5Na$, 493.2930) in the HR-ESI-MS. The IR absorption bands confirmed the presence of -OH (3380 cm^{-1}) and -COOH (1644 cm^{-1}) groups. The UV spectrum exhibited an absorption band at λ 204 (278 nm), corresponding to the carbonyl group. The 1H NMR spectrum (Table 1) showed an olefinic proton at δ_H 5.28 (1H, t, $J = 3.8$ Hz) and six methyl groups [δ_H 1.85, (3H, d, $J = 2.0$ Hz, H-23), 1.39 (3H, s, H-27), 1.14 (3H, s, H-29), 1.00 (3H, d, $J = 6.6$ Hz, H-30), 0.93 (3H, s, H-25), and 0.85 (3H, s, H-26)]. The ^{13}C NMR (Table 2) and DEPT 135 spectra revealed 29 signals, with a ketocarbonyl carbon at (δ_C 195.7), a carboxylic carbon at (δ_C 182.8), two double bonds at (δ_C 140.0, 128.1 and 145.3, 133.1), an oxygenated quaternary carbon at (δ_C 74.2), and six methyl carbons at (δ_C 29.5, 24.5, 17.7, 16.2, 14.4, and 13.4). The HMBC and 1H - 1H COSY correlations of compound **2** are illustrated in Figure 2. Meanwhile, an analysis of the 1H and ^{13}C NMR data of compound **2** established its close structural resemblance to 2-oxo-3 J ,19 α -dihydroxy-24-nor-urs-12-en-28-oic acid [27]. The only difference between the compound and the resemblance structure is the presence of a double bond at C-3/C-4 in compound **2**. It can be observed that the attachment of a double bond to C-3 and C-4 was established by the HMBC correlations from δ_H 2.56 and 2.16 (H-1) to δ_C 195.7 (C-2), δ_C 145.3 (C-3), δ_C 49.9 (C-5), and δ_C 39.3 (C-10) and from δ_H 1.00 (H₃-23) to δ_C 145.3 (C-3), δ_C 133.1 (C-4), and δ_C 49.9 (C-5). The relative configuration of compound **2** was determined based on a NOESY experiment. The NOESY correlations (Figure 3) of H₃-29/H-12/H₃-26 showed the J -orientation of H₃-29, which indicated that the hydroxy group at C-29 was α -oriented [28]. Thus, compound **2**'s structure was determined to be 2-oxo-3,19 α -dihydroxy-24-nor-urs-12-en-28-oic acid, and it was named oenothermalanosterol D. The data are available in supplementary materials.

Compound **3** (Figure 1) was isolated as a white amorphous powder (12.8 mg), possessing the molecular formula of $C_{30}H_{46}O_5$, based on HR-ESI-MS at m/z 509.3237 $[M + Na]^+$ (calculated for $C_{30}H_{46}O_5Na$, 509.3243). The IR absorption bands confirmed the presence of -OH (3368 cm^{-1}) and -COOH (1686 cm^{-1}) groups. The UV spectrum showed an absorption band at λ 204 nm, corresponding to the carbonyl group. The 1H NMR spectrum (Table 1) showed an olefinic proton at δ_H 5.27 (1H, t, $J = 3.6$ Hz, H-12), an oxygenated methine at δ_H 3.36 (1H, dd, $J = 4.6, 12.2$ Hz, H-3), and seven methyl groups [δ_H 0.86 (3H, s, H-26), 0.94

(3H, d, $J = 6.7$ Hz, H-30), 1.01 (3H, s, H-23), 1.04 (3H, s, H-24), 1.22 (3H, s, H-29), 1.32 (3H, s, H-25), and 1.36 (3H, s, H-27)]. The ^{13}C NMR (Table 2) and DEPT 135 spectra revealed 30 signals, with a ketocarbonyl carbon at (δ_{C} 215.3), a carboxylic carbon at (δ_{C} 182.2), a double bond at (δ_{C} 139.4 and 130.0), an oxygenated quaternary carbon at (δ_{C} 73.5), an oxygenated methine carbon at (δ_{C} 79.7), and seven methyl carbons at (δ_{C} 29.0, 27.0, 24.8, 18.1, 16.6, 16.6, and 15.9). Furthermore, an analysis of the ^{13}C NMR data of compound 3 established its close structural resemblance to 2-oxo-pomolic acid [29], which only differed in the position of the ketocarbonyl (δ_{C} 215.3, C-6) and replaced (δ_{C} 215.3, C-1) in the compound. The HMBC correlations from δ_{H} 3.10, 2.26 (H-2) to δ_{C} 215.3 (C-1), δ_{C} 79.7 (C-3), and δ_{C} 40.4 (C-4) were observed. The relative configuration of compound 3 was determined based on a NOESY experiment. The NOESY correlations (Figure 3) of H-3/H₃-23/H-5 demonstrated that the H-3 and H₃-23 were α -oriented, indicating the J -orientation of the hydroxy group at C-3. The correlations of H₃-29/H-12/H₃-26 demonstrated that H₃-29 was J -oriented, indicating the α -orientation of the hydroxy group at C-29 [30,31]. Thus, the structure of compound 3 was determined to be 3*J*,19*α*-dihydroxy-1-oxo-olean-12-en-28-oic acid, and it was named oenotheralanosterol E.

Compound 4 (Figure 1) was isolated as a white amorphous powder (11.7 mg), and its molecular formula was determined to be $\text{C}_{30}\text{H}_{46}\text{O}_6$, based on the quasi-molecular ion at m/z 525.3180 [$\text{M} + \text{Na}$]⁺ (calculated for $\text{C}_{30}\text{H}_{46}\text{O}_6\text{Na}$, 525.3192) in the HR-ESI-MS analysis. The IR absorption bands confirmed the presence of -OH (3366 cm^{-1}) and -COOH (1688 cm^{-1}) groups. The UV spectrum showed an absorption band at λ 203 nm, corresponding to the carbonyl group. The ^1H NMR (Table 1) and ^{13}C NMR (Table 2) data of compound 4 were similar to those of compound 3, differing only in the absence of a methyl group, which was replaced by an oxygenated methylene carbon (δ_{C} 66.0, C-23) in compound 4. The HMBC and ^1H - ^1H COSY correlations of compound 4 are illustrated in Figure 2. The HMBC correlations from δ_{H} 3.51, 3.35 (H₃-23) to δ_{C} 79.7 (C-3), δ_{C} 40.4 (C-4), δ_{C} 55.8 (C-5), and δ_{C} 13.3 (C-24) were observed. The relative configuration of compound 4 was determined based on a NOESY experiment. The NOESY correlations (Figure 3) of H-3/H₃-23/H-5 demonstrated that H-3 and H₃-23 were α -oriented, implying the J -orientation of the hydroxy group at C-3. The correlations of H₃-29/H-12/H₃-26 demonstrated the J -orientation of H₃-29, indicating the α -orientation of the hydroxy group at C-29 [32]. Thus, the structure of compound 4 was determined to be 3*J*,19*α*-dihydroxy-1-oxo-olean-12-en-23-ol-28-oic acid, and it was named oenotheralanosterol F.

Compound 5 (Figure 1) was isolated as a white amorphous powder (3.4 mg), and its molecular formula was established as $\text{C}_{28}\text{H}_{42}\text{O}_7$ from the molecular ion peak at m/z 513.2832 [$\text{M} + \text{Na}$]⁺ (calculated for $\text{C}_{28}\text{H}_{42}\text{O}_7\text{Na}$, 513.2828) in the HR-ESI-MS. The IR absorption bands confirmed the presence of -OH ($3371, 2951\text{ cm}^{-1}$) and -COOH ($1650, 1388\text{ cm}^{-1}$) groups. The UV spectrum exhibited an absorption band at λ 204 nm, corresponding to the carbonyl group. The ^1H NMR spectrum (Table 1) showed an olefinic bond at δ_{H} 5.35 (1H, t, $J = 3.8$ Hz, H-12), two oxygenated methines at [δ_{H} 3.22 (1H, d, $J = 3.8$ Hz, H-22) and 3.91 (1H, dd, $J = 4.4, 11.6$ Hz, H-19)], and six methyl groups at [δ_{H} 0.84 (3H, s, H-26), 0.97 (3H, s, H-29), 1.03 (3H, s, H-30), 1.09 (3H, s, H-25), 1.34 (3H, s, H-27), and 2.23 (3H, s, H-23)]. The ^{13}C NMR (Table 2) and DEPT 135 spectra revealed 28 signals, with a ketocarbonyl carbon at (δ_{C} 215.3), two carboxylic carbons at (δ_{C} 180.7 and 175.2), a double bond at (δ_{C} 143.8 and 125.1), two oxygenated methine carbons at (δ_{C} 72.4 and 82.0), and six methyl carbons at (δ_{C} 31.6, 28.8, 26.2, 25.2, 18.4, and 17.5). The HMBC and ^1H - ^1H COSY correlations of compound 1 are shown in Figure 2. Furthermore, an analysis of the ^1H and ^{13}C NMR data of compound 5 established its close structural resemblance to ivorengein B [33], and the only difference was that the oxygenated methine (δ_{C} 72.4, C-22) replaced the methylene signal (δ_{C} 32.5, C-22). The HMBC correlations from δ_{H} 3.91 (H-22) to δ_{C} 53.0 (C-17), δ_{C} 182.2 (C-28), and δ_{C} 38.0 (C-21) were observed. The relative configuration of compound 5 was determined based on a NOESY experiment. The NOESY correlations (see Figure 3) of H-22/H-18/H₃-27 showed that H-18 and H-22 were α -oriented, indicating the J -orientation of the hydroxy group at C-22. The correlations of H-19/H-12/H₃-26 showed that H-19 was J -oriented, indicating

the *a*-orientation of the hydroxy group at C-19 [34]. Thus, the structure of compound 5 was determined to be 19 α ,22 β -dihydroxy-4-oxo-3,24-dinor-2,4-secoolean-12-ene-2,28-dioic acid, and it was named oenotheralanosterol G.

In addition, the known compounds 6–12 were also obtained from the dichloromethane part of *O. biennis*. Comparing the NMR spectroscopic data of compounds 6–12 with the reported literature, the known compounds were identified as 2 α ,3 α ,19 α -trihydroxy-24-norurs4(23),12-dien-28-oic acid (6) [35], 3 β ,23-dihydroxy-1-oxo-olean-12-en-28-oic acid (7) [36], remangilone C (8) [37], knoxivalic acid A (9) [38], termichebulolide (10) [39], rosasecotriterpene A (11) [40], and rosanortriterpene C (12) [41], respectively.

The TGF- β 1-induced lung slice fibrosis model provided an experimental basis for the study of the pathological mechanism of PF and therapeutic drugs. In this paper, we used this model to explore the anti-pulmonary fibrosis activities of the isolated compounds through real-time cell analysis. The results indicated that compounds 1–2, 6, 8, and 11 significantly decreased the damage of BEAS-2B cells induced by TGF- β 1, with EC₅₀ values ranging from 4.7 μ M to 9.9 μ M (Table 3). It is speculated that these compounds may have potential activities against PF.

Table 3. Anti-pulmonary fibrosis activities of compounds 1–12 against BEAS-2B cell damage induced by TGF- β 1.

Group	EC ₅₀ (μ M)	Group	EC ₅₀ (μ M)
CON	NA	6	4.7
M	NA	7	53.3
Pirfenidone	12.7	8	7.9
1	8.4	9	NA
2	9.9	10	NA
3	48.3	11	9.6
4	NA	12	NA
5	NA		

Note: CON: Normal group; M: Model group; Pirfenidone: Positive control compound.

According to our experimental results, the lung-protective activities are influenced by multiple structural factors. For example, compound 6 exhibited the most effective anti-pulmonary fibrosis activities compared to the other compounds; therefore, the double bond at C-4/C-23 might be an active group that could increase the structures' activities. Similarly, compound 10 showed weaker anti-pulmonary fibrosis activities compared to the other compounds, which means the esterification of the carboxyl group at C-28 could decrease the compounds' activities.

3. Materials and Methods

3.1. General Procedures

The NMR spectra were recorded using a Bruker AVANCE III 500 nuclear magnetic resonance instrument and mass spectra was completed with a Bruker maxis HD time-of-flight mass spectrometer (Bruker, Germany). The UV and IR spectra were recorded on a Thermo EVO 300 spectrometer (Thermo, Waltham, MA, USA) and a Thermo Nicolet IS 10 spectrometer (Thermo, Waltham, MA, USA). The separation of compounds was achieved on an LC-52 HPLC (separation Beijing Technology, SP-5030 semi-preparative high-pressure infusion pump, UV200 detector, easy Chromchromatographic workstation, with a COSMOSIL C18-MS-II chromatographic column of 250 mm \times 20 mm, 5 μ m). A Multiskan MK3 microplate reader (Thermo Fisher, Waltham, MA, USA) was used in the bioassay, along with a carbon dioxide type 3111 incubator (Thermo, Waltham, MA, USA) and a Centrifuge-5804R high speed centrifuge (Eppendorf, Germany). Column chromatography (CC) was performed using an MCI gel CHP-20 (TOSOH Corp, Tokyo, Japan), a Sephadex LH-20 (40–70 mm, anAmersham Pharmacia Biotech AB, Uppsala, Sweden) and silica gel (200–300 mesh, Marine Chemical Industry, Qingdao, China). The chemical reagents were

supplied by the Beijing Chemical Plant (Beijing, China), and the RTCA from Agilent, Santa Clara, CA, USA and TGF-J1 from PeperoTech, Cranbury, NJ, USA.

3.2. Plant Material

The *Oenothera biennis* L. specimens were collected in August 2019 from the Funiu Mountains in Henan Province, China. The plants were identified and authenticated by *prof.* Cheng-ming Dong of the Henan University of Chinese Medicine. A voucher specimen (YJC-201908) was deposited in the Engineering and Technology Center for Chinese Medicine Development of Henan Province, Zhengzhou, China.

3.3. Extraction and Isolation

The air-dried *Oenothera biennis* L. (40.0 kg) was subjected to extraction with an aqueous solution containing 50% acetone of tissue fragmentation (two times each 85 L, overnight). The extract (3.3 kg) was dispersed in H₂O (15 L) and sequentially extracted with PE (10 × 15 L), CH₂Cl₂ (10 × 15 L), EtOAc (10 × 15 L), and *n*-BuOH (10 × 15 L). The CH₂Cl₂ part (49.6 g) was separated using silica gel column chromatography (CC, 12 × 130 cm) involving a mobile phase of PE/EtOAc (100:0 to 0:100, *v/v*), yielding 10 fractions (Fr.1–Fr.10).

Subfraction Fr.8 (2.47 g) was fractionally eluted via silica gel column containing PE/EtOAc (20:1 to 0:1, *v/v*), which yielded nine subfractions (Fr.8-1–Fr.8-9). Subfraction Fr.8-6 (536.0 mg) was repeatedly separated via silica gel column containing CH₂Cl₂/MeOH (50:1 to 10:1, *v/v*), yielding seven subfractions (Fr.8-6-1–Fr.8-6-7). Subfraction Fr.8-6-5 (356.5 mg) was applied to a Sephadex LH-20 column containing MeOH/H₂O (70:30, *v/v*), and the product was purified by semipreparative HPLC (MeOH/H₂O 66:34), yielding compound **5** (3.4 mg, *t_R* = 33.2 min) and compound **12** (16.2 mg, *t_R* = 36.0 min). Then, the subfraction Fr.8-9 (950.0 mg) was fractionally separated via silica gel column containing CH₂Cl₂/MeOH (100:1 to 10:1, *v/v*), yielding four subfractions (Fr.8-9-1–Fr.8-9-4). Then, subfraction Fr.8-9-3 (251.6 mg) was fractionally separated via silica gel column containing CH₂Cl₂/MeOH (50:1 to 10:1, *v/v*) and purified using semipreparative HPLC (MeOH/H₂O = 66:34), yielding compound **1** (20.6 mg, *t_R* = 35.7 min) and compound **2** (11.0 mg, *t_R* = 50.4 min). The subfraction Fr.8-9-4 (341.5 mg) was chromatographed with Sephadex LH-20 MeOH/H₂O (70:30, *v/v*) and purified using semipreparative HPLC (MeOH/H₂O = 62:38), yielding compound **6** (14.7 mg, *t_R* = 29.1 min) and compound **10** (4.6 mg, *t_R* = 34.0 min). Sequentially, the subfraction Fr.8-9-5 (208.5 mg) was separated via silica gel column containing CH₂Cl₂/MeOH (40:1 to 5:1, *v/v*) and purified using semipreparative HPLC (MeOH/H₂O = 53:47), which yielded compound **7** (33.8 mg, *t_R* = 33.0 min).

In addition, subfraction Fr.9 (1.58 g) was fractionally separated via silica gel column containing CH₂Cl₂/MeOH (100:1 to 0:100, *v/v*), which yielded five subfractions (Fr.9-1–Fr.9-5). Then, the subfraction Fr.9-4 (0.78 g) was separated via silica gel column containing CH₂Cl₂/MeOH (50:1 to 10:1, *v/v*), yielding four subfractions (Fr.9-4-1–Fr.9-4-4). Further separation of the subfraction Fr.9-4-3 (304.2 mg) was chromatographed with Sephadex LH-20 MeOH/H₂O (70:30, *v/v*) and purified using semipreparative HPLC (MeOH/H₂O 65:35), producing compound **4** (11.7 mg, *t_R* = 30.6 min) and compound **3** (12.8 mg, *t_R* = 37.5 min). Meanwhile, subfraction Fr.9-4-4 (315.2 mg) was eluted via an MCI gel CHP-20 CC containing MeOH/H₂O (0:100 to 100:0, *v/v*), yielding nine fractions (Fr.9-4-4-1–Fr.9-4-4-4). Then, subfraction Fr.9-4-4-2 (194.2 mg) was separated via silica gel column containing CH₂Cl₂/MeOH (40:1 to 10:1, *v/v*) and purified with semipreparative HPLC (MeOH/H₂O 70:30), yielding compound **8** (26.4 mg, *t_R* = 31.3 min) and compound **9** (23.9 mg, *t_R* = 40.2 min). Subsequently, the subfraction Fr.9-5 (0.45 g) was separated via silica gel column containing CH₂Cl₂/MeOH (50:1 to 1:1, *v/v*), which yielded four subfractions (Fr.9-5-1–Fr.9-5-4). A Sephadex LH-20 column with MeOH/H₂O (70:30, *v/v*) was further used to separate the subfraction Fr.9-5-2 (235.1 mg), and the obtained product was purified with semipreparative HPLC (MeOH/H₂O = 48:52), which yielded compound **11** (12.8 mg, *t_R* = 28.1 min).

Oenotheralanosterol C (1): The white amorphous powder of compound 1 was characterized with $[\alpha]_D^{20} - 71.397$ (c 0.4120, CH₃OH), mp 217 °C, HR-ESI-MS m/z : 511.3397 [M + Na]⁺ (calculated for C₃₀H₄₈O₅Na, 511.3399) UV λ_{\max} (CH₃OH)/nm (log ϵ): 206 nm; IR (CH₃OH) ν_{\max} : 3369, 1636, 1457, 1019, and 682 cm⁻¹. ¹H NMR (500 MHz, CD₃OD) data can be found in Table 1 and ¹³C NMR (125 MHz, CD₃OD) data can be found in Table 2.

Oenotheralanosterol D (2): The white amorphous powder of compound 2 was characterized with $[\alpha]_D^{20} + 100.290$ (c 0.2192, CH₃OH), mp 238 °C, HR-ESI-MS m/z : 493.2934 [M + Na]⁺ (calculated for C₂₉H₄₂O₅Na, 493.2930) UV λ_{\max} (CH₃OH)/nm (log ϵ): 278, 204 nm; IR (CH₃OH) ν_{\max} : 3380, 1644, 1457, 1397, 1018, and 699 cm⁻¹. ¹H NMR (500 MHz, CD₃OD) data can be found in Table 1 and ¹³C NMR (125 MHz, CD₃OD) data can be found in Table 2.

Oenotheralanosterol E (3): The white amorphous powder of compound 3 was characterized with $[\alpha]_D^{20} + 69.888$ (c 0.2336, CH₃OH), mp 247 °C, HR-ESI-MS m/z : 509.3237 [M+Na]⁺ (calculated for C₃₀H₄₆O₅Na, 509.3243) UV λ_{\max} (CH₃OH)/nm (log ϵ): 204 nm; IR (CH₃OH) ν_{\max} : 3368, 2941, 1686, 1459, 1383, 1238, 1018, 656, 603, and 557 cm⁻¹. ¹H NMR (500 MHz, CD₃OD) data can be found in Table 1 and ¹³C NMR (125 MHz, CD₃OD) data can be found in Table 2.

Oenotheralanosterol F (4): The white amorphous powder of compound 4 was characterized with $[\alpha]_D^{20} + 62.971$ (c 0.2552, CH₃OH), mp 246 °C, HR-ESI-MS m/z : 525.3180 [M+Na]⁺ (calculated for C₃₀H₄₆O₆Na, 525.3192) UV λ_{\max} (CH₃OH)/nm(log ϵ): 203 nm; IR (CH₃OH) ν_{\max} : 3366, 2939, 1688, 1455, 1385, 1239, 1021, and 655 cm⁻¹. ¹H NMR (500 MHz, CD₃OD) data can be found in Table 1 and ¹³C NMR (125 MHz, CD₃OD) data can be found in Table 2.

Oenotheralanosterol G (5): The white amorphous powder of compound 4 was characterized with $[\alpha]_D^{20} + 62.971$ (c 0.2552, CH₃OH), mp 219 °C, HR-ESI-MS m/z : 513.2832 [M+Na]⁺ (calculated for C₂₈H₄₂O₇Na, 513.2828) UV λ_{\max} (CH₃OH) /nm(log ϵ): 204 nm; IR (CH₃OH) ν_{\max} : 3371, 2951, 1650, 1388, 1202, 1018, 669, and 554 cm⁻¹. ¹H NMR (500 MHz, CD₃OD) data can be found in Table 1 and ¹³C NMR (125 MHz, CD₃OD) data can be found in Table 2.

3.4. In Vitro Cell Experiment

In the previous stage, the research group conducted relevant studies on the anti-pulmonary fibrosis activities of the total extracts and some monomers of *Oenothera biennis* L. Based on this, the RTCA method was used to detect the effect of monomer compounds on TGF- β 1-induced BEAS-2B cell damage to explore its anti-pulmonary fibrosis active ingredients.

An xCELLigence instrument (Acea Biosciences, Inc., San Diego, CA, USA) was used for the real-time cell analysis (RTCA) assay. BEAS-2B cells were plated in 16-well plates (2.5 × 10⁴ cells/well) for 24 h at 37 °C in a humidified atmosphere of 5% CO₂. Then, these compounds, or pirfenidone at various concentrations (0.1, 1, 10, 50, and 100 μ M), were added to the standard medium of TGF- β 1 (1 ng/mL) and incubated for 24 h. Each experiment was repeated four times to obtain the mean values. Finally, the EC₅₀ values of these compounds were calculated by GraphPadSigmoidal dose-response.

4. Conclusions

In conclusion, we successfully isolated five new triterpenoids and seven known compounds from *Oenothera biennis* L. The bioassay indicated that compounds 1–2, 6, 8, and 11 exhibited significant anti-pulmonary fibrosis activities to TGF- β 1-induced BEAS-2B cells, with EC₅₀ values ranging from 4.7 μ M to 9.9 μ M. These results provide a certain theoretical basis for the further development and utilization of *Oenothera biennis* L.

Supplementary Materials: The following supporting information can be downloaded at: <https://www.mdpi.com/article/10.3390/molecules27154870/s1>. The 1D, 2D NMR, and HR-ESI-MS spectra of compounds 1–12 are available in the supplementary data.

Author Contributions: J.L., separation of compounds, structural identification, and writing—original draft. J.Z., separation of compounds. M.Z., study of the anti-pulmonary fibrosis activity of the compounds. M.L., S.X., X.Z. and W.F., writing—review and editing, structural identification, methodology. All authors have read and agreed to the published version of the manuscript.

Funding: This work was financially supported by The Major Science and Technology Projects in Henan Province (171100310500), the National Key Research and Development Project (2019YFC1708802), the National Natural Science Foundation of China (82104386), and the Scientific and technological key project in Henan Province (212102310345).

Institutional Review Board Statement: Not applicable.

Informed Consent Statement: Not applicable.

Data Availability Statement: The data presented in this study are available on request from the corresponding author.

Conflicts of Interest: There is no conflict of interest to declare.

Sample Availability: Samples of the compounds are not available from the authors.

References

1. Deng, L.; Zhou, X.Q.; Jian, D.J. Progress in evaluation and development of drugs for treatment of pulmonary fibrosis. *Chin. J. New Drugs* **2021**, *30*, 712–717.
2. Spagnolo, P.; Balestro, E.; Aliberti, S. Pulmonary fibrosis secondary to COVID-19: A call to arms? *Lancet Respir. Med.* **2020**, *8*, 750–752. [[CrossRef](#)]
3. Vancheri, C.; Kreuter, M.; Richeldi, L. Nintedanib with add-on pirfenidone in idiopathic pulmonary fibrosis. Results of the INJOURNEY Trial. *Am. J. Respir. Crit. Care Med.* **2018**, *197*, 356–363. [[CrossRef](#)]
4. Liu, M.W.; Su, M.X.; Tang, D.Y. Ligustrazin increases lung cell autophagy and ameliorates paraquat-induced pulmonary fibrosis by inhibiting PI3K/Akt/mTOR and hedgehog signalling via increasing miR-193a expression. *BMC Pulm. Med.* **2019**, *19*, 35. [[CrossRef](#)]
5. Zhang, R.; Xu, L.M.; An, X.X.; Sui, X.B.; Lin, S. Astragalus polysaccharides attenuate pulmonary fibrosis by inhibiting the epithelial-mesenchymal transition and NF- κ B pathway activation. *Int. J. Mol. Med.* **2020**, *46*, 331–339. [[CrossRef](#)]
6. Thomas, D.; Anandasadagopan, S.; Ganapasam, S. Autophagy induction by celastrol augments protection against bleomycin-induced experimental pulmonary fibrosis in rats: Role of adaptor protein p62/SQSTM1. *Pulm. Pharmacol. Ther.* **2017**, *45*, 47–61.
7. Chen, J.H.; Shi, Y.Y.; He, L.; Hao, H.R.; Wang, B.L.; Zheng, Y.L.; Hu, C.P. Protective roles of polysaccharides from *Ganoderma lucidum* on bleomycin-induced pulmonary fibrosis in rats. *Int. J. Biol. Macromol.* **2016**, *92*, 278–281. [[CrossRef](#)]
8. Liu, J.; Huang, Y.; Zhang, L.; Yang, Y.R.; Sun, J.; Yu, S.X.; Li, J. Preventive effect of triterpene acids of loquat on lipid peroxidation of pulmonary fibrosis on rats. *Acta Univ. Med. Anhui* **2010**, *45*, 50–53.
9. Xu, Y.Q.; Li, H.Y.; Hu, B.Z. Research progress of *Oenothera* L. plants. *J. Northeast Agric. Univ.* **2006**, *37*, 111–114.
10. Granica, S.; Czerwi', N.; Piwowarski, J.P.; Ziaja, M.; Kiss, A.K. Chemical composition, antioxidative and anti-inflammatory activity of extracts prepared from aerial parts of *Oenothera biennis* L. and *Oenothera paradoxa* Hudziok obtained after seeds cultivation. *J. Agric. Food Chem.* **2013**, *61*, 801–810. [[CrossRef](#)]
11. Singh, S.; Kaur, R.; Sharma, S.K. An updated review on the *Oenothera* genus. *J. Chin. Integr. Med.* **2012**, *10*, 717–725. [[CrossRef](#)] [[PubMed](#)]
12. Ahmad, A.; Singh, D.K.; Fatima, K.; Tandon, S.; Luqman, S. New constituents from the roots of *Oenothera biennis* and their free radical scavenging and ferric reducing activity. *Ind. Crops Prod.* **2014**, *58*, 125–132. [[CrossRef](#)]
13. Christie, W.W. The analysis of evening primrose oil. *Ind. Crops Prod.* **1999**, *10*, 73–83. [[CrossRef](#)]
14. Barre, D.E. Potential of evening primrose, borage, black currant, and fungal oils in human health. *Ann. Nutr. Metab.* **2001**, *45*, 47–57. [[CrossRef](#)]
15. Wang, H.Q.; Cui, H.Z.; Li, C.; Chen, S.S.; Nielu, S.N. Evening primrose oil regulates p38MAPK and NF- κ B signaling pathway for anti-inflammatory treatment of acne. *Pharmacol. Clin. Chin. Mater. Med.* **2018**, *34*, 62–67.
16. Liu, S.L. Ultrasonic-Assisted Extraction, Purification and Antioxidant Activity of Polysaccharides from Evening Primrose (*Oenothera biennis* L.) Leaves. Master's Thesis, Jilin University, Changchun, China, 2018.
17. Mert, H.D.; Irak, K.V.; Cibuk, S.L.; Yildirim, S.K.; Mert, N.H. The effect of evening primrose oil (*Oenothera biennis*) on the level of adiponectin and some biochemical parameters in rats with fructose induced metabolic syndrome. *Arch. Physiol. Biochem.* **2020**, *1–9*. [[CrossRef](#)]
18. Fukushima, M.; Ohhashi, T.; Ohno, S.; Saitoh, H.; Sonoyama, K. Effects of diets enriched in n-6 or n-3 fatty acids on cholesterol metabolism in older rats chronically fed a cholesterol-enriched diet. *Lipids* **2001**, *36*, 261–266. [[CrossRef](#)]
19. Nicolaou, A. Eicosanoids in skin inflammation. *Prostaglandins Leukot. Essent. Fat. Acids* **2013**, *88*, 131–138. [[CrossRef](#)]

20. Ras, R.T.; Geleijnse, J.M.; Trautwein, E.A. LDL-cholesterol-lowering effect of plant sterols and stanols across different dose ranges: A metaanalysis of randomized controlled studies. *Br. J. Nutr.* **2014**, *112*, 214–219. [[CrossRef](#)]
21. Das, U.N.; Rao, K.P. Effect of γ -linolenic acid and prostaglandins E1 on gamma-radiation and chemical-induced genetic damage to the bone marrow cells of mice. *Prostaglandins Leukot. Essent. Fat. Acids* **2006**, *74*, 165–173. [[CrossRef](#)]
22. Yu, S.Q.; Tian, Y.Q. Research progress on breeding, development and cultivation of evening primrose in our country. *Chin. Tradit. Herb. Drugs* **2000**, *1*, 72–74.
23. Shilpi, S.; Vijaya, D.; Dhananjay, K.S.; Kaneez, F.; Ateeque, A.; Suaib, L. Antiproliferative and antimicrobial efficacy of the compounds isolated from the roots of *Oenothera biennis* L. *J. Pharm. Pharmacol.* **2017**, *69*, 1230–1243.
24. Zeng, N.; Shen, Y.; Li, L.Z.; Jiao, W.H.; Gao, P.Y.; Song, S.J.; Chen, W.S. Anti-inflammatory Triterpenes from the Leaves of *Rosa laevigata*. *J. Nat. Prod.* **2011**, *74*, 732–738. [[CrossRef](#)] [[PubMed](#)]
25. Ouyang, J.K.; Dong, L.M.; Xu, Q.L.; Wang, J.; Liu, S.B.; Qian, T.; Yuan, Y.F.; Tan, J.W. Triterpenoids with α -glucosidase inhibitory activity and cytotoxic activity from the leaves of *Akebia trifoliata*. *RSC Adv.* **2018**, *8*, 40483–40489. [[CrossRef](#)]
26. Wang, J.; Ren, H.; Xu, Q.L.; Zhou, Z.Y.; Wu, P.; Wei, X.Y.; Cao, Y.; Chen, X.X.; Tan, J.W. Antibacterial oleanane-type triterpenoids from pericarps of *Akebia trifoliata*. *Food Chem.* **2015**, *168*, 623–629. [[CrossRef](#)]
27. Parichat, N.; Wolfgang, K.; Uwe, B.; Juergen, C.; Iris, K.; Somyote, S. Novel 24-nor-, 24-nor-2,3-seco-, and 3,24-dinor-2,4-seco-ursane triterpenes from *Diospyros decandra*: Evidence for ring A biosynthetic transformations. *Tetrahedron* **2006**, *62*, 5519–5526.
28. Louis, P.S.; Abdou, T.; Hippolyte, N.N.; Mehdi, Y.; Enrico, P.; Felix, K.; Francois, C.; Gilbert, K.; Bonaventure, T.N. New Nortriterpenoid and Ceramides From Stems and Leaves of Cultivated *Triumfetta cordifolia* A Rich (Tiliaceae). *J. Am. Oil Chem. Soc.* **2010**, *87*, 1167–1177.
29. Lv, K.Y.; Li, J.Y.; Wang, C.L.; He, L.S.; Quan, S.; Zhang, J.Z.; Liu, D.L. Triterpenoids from *Rosa odorata* Sweet var. *gigantea* (Coll. et Hemsl.) Rehd. et Wils and their chemotaxonomic significance. *Biochem. Syst. Ecol.* **2021**, *96*, 104240. [[CrossRef](#)]
30. Srinivasa, C.P.; Adeyemi, O.A.; Lenka, P.S.; Lucie, R.; Jiří, G.; Karel, D.; Johannes, V.S. Identification and characterisation of potential bioactive compounds from the leaves of *Leucosidea sericea*. *J. Ethnopharmacol.* **2018**, *220*, 169–176.
31. Chen, Z.Z.; Tong, L.; Feng, Y.L.; Wu, J.Z.; Zhao, X.Y.; Ruan, H.L.; Pi, H.F.; Zhang, P. Ursane-type nortriterpenes with a five-membered A-ring from *Rubus inominatus*. *Phytochem.* **2015**, *116*, 329–336. [[CrossRef](#)]
32. Mariko, K.; Hashimoto, K.I.; Masashi, Y.; Hiromitsu, T.; Norio, A. Two New 19-Hydroxyursolic Acid-type Triterpenes from Peruvian 'Unã de Gato' (*Uncaria tomentosa*). *Tetrahedron* **2000**, *56*, 547–552.
33. Beaudelaire, K.P.; Rémy, B.T.; Massimo, R.; Téléphore, B.N.; Luana, Q.; Massimo, B.; Giulio, L.; Luciano, B.; Léon, A.T. Novel 3-Oxo- and 3,24-Dinor-2,4-secooleanane-Type Triterpenes from *Terminalia ivorensis*, A. Chev. *Chem. Biodivers.* **2011**, *8*, 1301–1309.
34. Michał, G.; Marta, K.D.; Agata, R.; Maciej, W.; Izabela, F. Triterpenoids from strawberry *Fragaria × ananassa* Duch. cultivar Senga Sengana leaves. *Ind. Crops Prod.* **2021**, *169*, 113668.
35. Dae, S.J.; Jong, M.K.; Joo, H.K.; Jin, S.K. 24-nor-Ursane Type Triterpenoids from the Stems of *Rumex japonicas*. *Chem. Pharm. Bull.* **2005**, *53*, 1594–1596.
36. Lai, Y.C.; Chen, C.K.; Tsai, S.F.; Lee, S.S. Triterpenes as α -glucosidase inhibitors from *Fagus hayatae*. *Phytochemistry* **2012**, *74*, 206–211. [[CrossRef](#)]
37. Deng, Y.H.; Jiang, T.Y.; Sheng, S.J.; Manoelson, T.R.; Snyder, J.K. Remangilonones A-C, New Cytotoxic Triterpenes from *Physenamadagascariensis*. *J. Nat. Prod.* **1999**, *62*, 471–476. [[CrossRef](#)]
38. Zhao, F.; Ma, L.; Sun, J.F.; Han, J.T.; Wang, Y.F.; Zhang, S.P. A new nor-triterpenoid from root tubers of *Knoxia valerianoides*. *Chin. Tradit. Herb. Drugs.* **2014**, *45*, 28–30.
39. Zhang, C.; Jiang, K.; Qu, S.J.; Zhai, Y.M.; Tan, J.J.; Tan, C.H. Triterpenoids from the barks of *Terminalia chebula*. *J. Asian Nat. Prod. Res.* **2015**, *17*, 996–1001. [[CrossRef](#)]
40. Liu, Y.H.; Tian, Y.Y.; Long, H.; Li, G.; Liu, Z.X.; Wei, H. A new seco-triterpene from roots of *Rosa laevigata*. *Chin. Tradit. Herb. Drugs* **2018**, *49*, 5740–5745.
41. Tian, Y.N.; Feng, L.; Li, B.L.; Hu, J.J.; Xie, J.D.; Xiao, W.J.; Nie, L.H.; Wu, J.W. Rosanortriterpene C, a 3,24-Dinor-2,4-seco-ursane Triterpene from the Fruits of *Rosa laevigata* var. *leiocapus*. *Chem. Pharm. Bull.* **2019**, *67*, 1255–1258. [[CrossRef](#)]